Article

Oligo(*p*-phenylenevinylene)#Peptide Conjugates: Synthesis and Self-Assembly in Solution and at the Solid#Liquid Interface

Rachid Matmour, Inge De Cat, Subi J. George, Wencke Adriaens, Philippe Lecle#re, Paul H. H. Bomans, Nico A. J. M. Sommerdijk, Jeroen C. Gielen, Peter C. M. Christianen, Jeroen T. Heldens, Jan C. M. van Hest, Dennis W. P. M. Lo#wik, Steven De Feyter, E. W. Meijer, and Albertus P. H. J. Schenning

J. Am. Chem. Soc., **2008**, 130 (44), 14576-14583 • DOI: 10.1021/ja803026j • Publication Date (Web): 11 October 2008

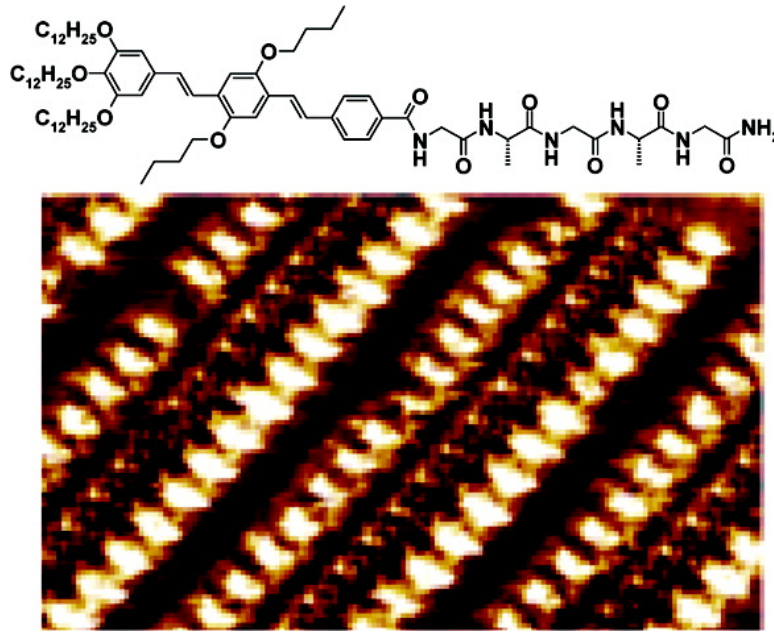

More About This Article

Additional resources and features associated with this article are available within the HTML version:

- Supporting Information
- Access to high resolution figures
- Links to articles and content related to this article
- Copyright permission to reproduce figures and/or text from this article

View the Full Text HTML

J|A|C|S
ARTICLES

Published on Web 10/11/2008

Oligo(*p*-phenylenevinylene)−Peptide Conjugates: Synthesis and Self-Assembly in Solution and at the Solid−Liquid Interface

Rachid Matmour,[†,▽] Inge De Cat,[‡] Subi J. George,[†] Wencke Adriaens,[†] Philippe Leclère,[†,§] Paul H. H. Bomans,[||] Nico A. J. M. Sommerdijk,[||] Jeroen C. Gielen,[⊥] Peter C. M. Christianen,[⊥] Jeroen T. Heldens,[#] Jan C. M. van Hest,[#] Dennis W. P. M. Löwik,[#] Steven De Feyter,*[,‡] E. W. Meijer,*[,†] and Albertus P. H. J. Schenning*[,†]

Laboratory of Macromolecular and Organic Chemistry, Eindhoven University of Technology, P.O. Box 513, 5600 MB Eindhoven, The Netherlands, Division of Molecular and Nano Materials, Department of Chemistry and INPAC, Institute of Nanoscale Physics and Chemistry, Katholieke Universiteit Leuven, Celestijnenlaan 200F, B-3001 Leuven, Belgium, Service de Chimie des Matériaux Nouveaux, Université de Mons-Hainaut, Place du Parc 20, B-7000 Mons, Belgium, Soft Matter CryoTEM Research Unit, Eindhoven University of Technology, P.O. Box 513, 5600 MB Eindhoven, The Netherlands, IMM, High Field Magnet Laboratory, HFML, Radboud University of Nijmegen, Toernooiveld 7, 6525 ED, Nijmegen, The Netherlands, and Bio-Organic Chemistry, Institute for Molecules and Materials, Radboud University Nijmegen, Heyendaalseweg 135, 6525 AJ, Nijmegen, The Netherlands

Received April 24, 2008; E-mail: steven.defeyter@chem.kuleuven.be; e.w.meijer@tue.nl; a.p.h.j.schenning@tue.nl

Abstract: Two oligo(*p*-phenylenevinylene)−peptide hybrid amphiphiles have been synthesized using solid- and liquid-phase strategies. The amphiliphiles are composed of a π-conjugated oligo(*p*-phenylenevinylene) trimer (OPV) which is coupled at either a glycinyl-alanyl-glycinyl-alanyl-glycine (GAGAG) silk-inspired β-sheet or a glycinyl-alanyl-asparagyl-prolyl-asparagy-alanyl-alanyl-glycine (GANPNAAG) β-turn forming oligopeptide sequence. The solid-phase strategy enables one to use longer peptides if strong acidic conditions are avoided, whereas the solution-phase coupling gives better yields. The study of the two-dimensional (2D) self-assembly of OPV−GAGAG by scanning tunneling microscopy (STM) at the submolecular level demonstrated the formation of bilayers in which the molecules are lying antiparallel in a β-sheet conformation. In the case of OPV−GANPNAAG self-assembled monolayers could not be observed. Absorption, fluorescence, and circular dichroism studies showed that OPV−GAGAG and OPV−GANPNAAG are aggregated in a variety of organic solvents. In water cryogenic temperature transmission electron microscopy (cryo-TEM), atomic force microscopy (AFM), light scattering, and optical studies reveal that self-assembled nanofibers are formed in which the helical organization of the OPV segments is dictated by the peptide sequence.

Introduction

Self-assembly is regarded as a practical and promising approach for building a wide variety of functional, complex nanostructures.[1] Among the large diversity of molecules that form ordered supramolecular nanostructures, peptide amphiphiles[2−5] constitute an interesting class. Peptide amphiphiles comprise a hydrophilic peptide sequence and a hydrophobic part that can be an aliphatic tail or again a peptide tail.[6] Due to the information that is present in the peptide sequence a diverse set of assemblies having a distinct secondary and tertiary structure have been designed.[7] Peptide-based systems can have various bionanotechnological applications such as supports for functional and responsive materials and sensors.[8,9]

Another category that has received a lot of attention in the area of supramolecular nanostructures is self-assembled π-conjugated oligomers. Such systems are appealing to influence and control the morphology in electronic devices and for the construction of nanowires.[10] Furthermore, π-conjugated oligomers are excellent probes to study self-assembly mechanisms and to obtain knowledge about phase behavior and dynamics of multicomponent systems.[11]

Combining π-conjugated oligomers with peptides seems an attractive approach to obtain exact two-dimensional (2D) and three-dimensional (3D) spatial orientation and packing of π-conjugated oligomers in which the orientation and packing is dictated by the peptide sequence.[12,13] Moreover, the use of these π-conjugated materials to transduce molecular recognition

[†] Laboratory of Macromolecular and Organic Chemistry, Eindhoven University of Technology.
[‡] Katholieke Universiteit Leuven.
[§] Université de Mons-Hainaut.
[||] Soft Matter CryoTEM Research Unit, Eindhoven University of Technology.
[⊥] High Field Magnet Laboratory, Radboud University of Nijmegen.
[#] Institute for Molecules and Materials, Radboud University Nijmegen.
[▽] Present address: Polymer Research, MICHELIN group, Place des Carmes-Déchaux, 63040 Clermont-Ferrand Cedex 9, France.

 10.1021/ja803026j CCC: $40.75

Scheme 1. Synthesis of **OPV-1** and **OPV-2**[a]

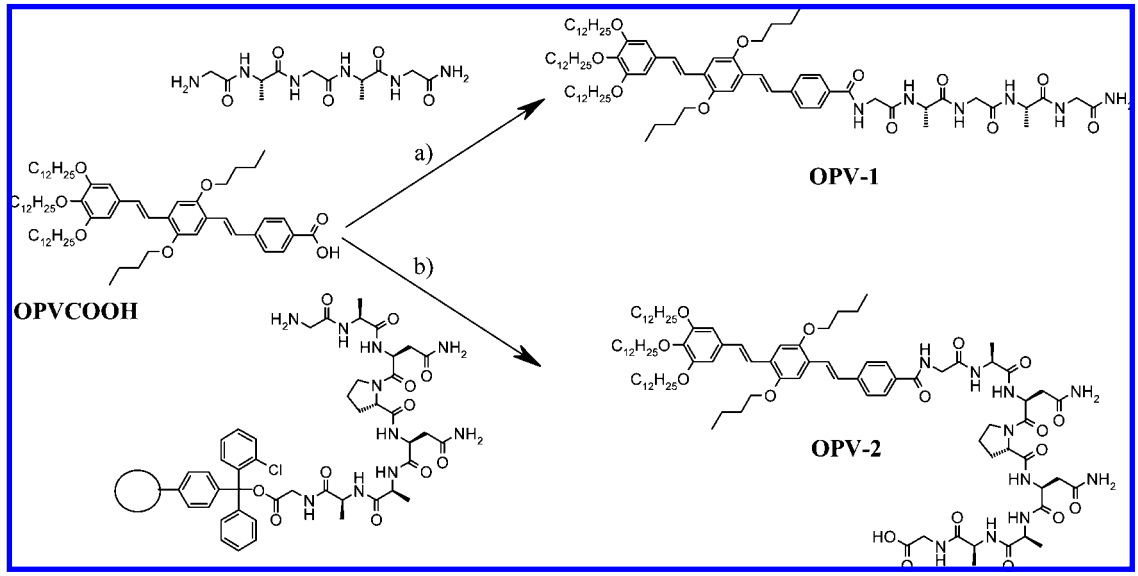

[a] (a) HBTU/DIPEA, DMF/DCM, 62%; (b) (1) DIPCDI/HOBt, DCM/DMF, (2) TFE/HOAc, DCM, 28%.

by the peptide segment into an electronic or optical signal would be of interest.[14] The π-conjugated element can in principle also be used as an optical probe to study the self-assembly mechanisms of peptides.[15] The self-assembly of π-conjugated polymer and oligomer peptide conjugates is, however, nearly unexplored. The bulk organization of triblock copolymers containing polyfluorene and poly(γ-benzyl-L-glutamate) segments has been reported.[16] In case of oligomers, the solid-state self-assembly of a peptide-functionalized tetrathiophene[17] and the aqueous supramolecular aggregates of an L-lysine branched phenyl vinylene derivative have been described,[18] while an oligo(phenylen-ethynylene) template has been used to organize oligopeptides.[19] Amphiphilic peptide assemblies with a π-conjugated polydiacetylene backbone,[20] templated assemblies,[21] and π-conjugated polymer peptide conjugates[22] for mainly sensing applications have been reported, whereas also dye peptide conjugates are known.[23]

Here, we report the synthesis and self-assembly of two π-conjugated oligomer−peptide conjugates, that is, an oligo(*p*-phenylenevinylene) (OPV)[24] functionalized by a glycinyl-alanyl-glycinyl-alanyl-glycine (GAGAG) or a glycinyl-alanyl-asparagyl-prolyl-asparagy-alanyl-alanyl-glycine (GANPNAAG) peptide sequence (Scheme 1). We chose a simple GAGAG pentapeptide sequence since the AlaGly motif has been identified as an important basic repeat sequence in the crystalline β-sheet domains.[25] The second peptide we studied contains the NPNA sequence found in the CS protein of the malaria, *Plasmodium falciparum*.[26] It is repeated over 40 times and proposed to be in a β-hairpin-like structure, an important folding motif that is ubiquitous in molecular recognition events and biological activity of proteins.[27] Furthermore, peptide amphiphiles containing the GANPNAAG peptide sequence have been reported forming helically twisted bilayer ribbons in which the peptides arranged in a β-sheet.[28] The OPV−peptide conjugates can be self-assembled in organic and aqueous media as well as at the solid−liquid interface.

Results and Discussion

Synthesis of the OPV−Peptide Conjugates. The synthesis of the OPV−peptide conjugates, **OPV-1** and **OPV-2** was performed by coupling of oligo(*p*-phenylenevinylene) carboxylic acid derivative **OPV−COOH** with the N-terminated amine peptides (Scheme 1). **OPV−COOH** was prepared according to a literature procedure.[29] The GAGAG peptide, possessing an amine and an amide at the N-terminus and C-terminus, respectively, was synthesized by standard *tert*-butyloxycarbonyl (Boc)-mediated solid-phase peptide synthesis on a 4-methylbenzhydrylamine (MBHA) resin.[28] After cleavage from the resin, the GAGAG pentapeptide sequence was purified by reversed-phase high-performance liquid chromatography (RP-HPLC). The amino-terminated GANPNAAG was conveniently prepared on a chlorotrityl (Barlos) resin using standard solid-phase 9-fluorenylmethoxycarbonyl (Fmoc) chemistry.[30] The liquid-phase coupling reaction of the **OPV−COOH** with the GAGAG peptide sequence was preferred to the solid-phase synthesis to avoid any degradation of the π-conjugated system during the resin cleavage step with strong acids such as trifluoroacetic acid (TFA). **OPV−COOH** was first activated by *O*-(benzotriazol-1-yl)-*N*,*N*,*N*′,*N*′-tetramethyluronium hexafluorophosphate (HBTU) and diisopropylethylamine (DIPEA) and then treated with the amine-terminated GAGAG peptide (Scheme

(1) Service, F. *Science* **2005**, *309*, 9.
(2) (a) Paramonov, S. E.; Jun, H.-W.; Hartgerink, J. D. *J. Am. Chem. Soc.* **2006**, *128*, 7291. (b) Stendahl, J. C.; Rao, M. S.; Guler, M. O.; Stupp, S. I. *Adv. Funct. Mater.* **2006**, *16*, 499. (c) Zhang, S.; Holmes, T.; Lockshin, C.; Rich, A. *Proc. Natl. Acad. Sci. U.S.A.* **1993**, *90*, 3334. (d) Behanna, H. A.; Donners, J. J. J. M.; Gordon, A. C.; Stupp, S. I. *J. Am. Chem. Soc.* **2005**, *127*, 1193.
(3) (a) Rapaport, H.; Kjaer, K.; Jensen, T. R.; Leiserowitz, L.; Tirrell, D. A. *J. Am. Chem. Soc.* **2000**, *122*, 12523. (b) Powers, E. T.; Yang, S. I.; Lieber, C. M.; Kelly, J. W. *Angew. Chem., Int. Ed.* **2002**, *41*, 127. (c) Xu, G.; Wang, W.; Groves, J. T.; Hecht, M. H. *Proc. Natl. Acad. Sci. U.S.A.* **2001**, *98*, 3652. (d) Schneider, J. P.; Pochan, D. J.; Ozbas, B.; Rajagopal, K.; Pakstis, L.; Kretsinger, J. *J. Am. Chem. Soc.* **2002**, *124*, 15030. (e) Bong, D. T.; Clark, T. D.; Granja, J. R.; Ghadiri, M. R. *Angew. Chem., Int. Ed.* **2001**, *40*, 988.
(4) (a) Yu, Y. C.; Berndt, P.; Tirrell, M.; Fields, G. B. *J. Am. Chem. Soc.* **1996**, *118*, 12515. (b) Berndt, P.; Fields, G. B.; Tirrell, M. *J. Am. Chem. Soc.* **1995**, *117*, 9515. (c) Hartgerink, J. D.; Beniash, E.; Stupp, S. I. *Science* **2001**, *294*, 1684. (d) Hartgerink, J. D.; Beniash, E.; Stupp, S. I. *Proc. Natl. Acad. Sci. U.S.A.* **2002**, *99*, 5133. (e) Silva, G. A.; Czeisler, C.; Niece, K. L.; Beniash, E.; Harrington, D. A.; Kessler, J. A.; Stupp, S. I. *Science* **2004**, *303*, 1352.

1). After purification, **OPV-1** was obtained in 62% yield. A similar solution-phase coupling of *N*-hydroxysuccinimide ester of **OPV−COOH** with fully deprotected GANPNAAG failed due to poor solubility of the peptide. Therefore, **OPV-2** was synthesized on the solid phase (Scheme 1). To avoid strongly acidic conditions, the Barlos resin was employed that allows cleavage with trifluoroethanol/acetic acid in dichloromethane. Moreover, the peptide was synthesized without any protective groups on the asparagine residues which are normally protected with a trityl group and need to be removed with 95% TFA. Any attempt to remove these trityl groups from the OPV−GANPNAAG conjugate was accompanied with degradation of the final product. To reduce any dehydration of the asparagines upon activation these residues were introduced using the corresponding pentafluorophenol ester instead of employing a diisopropylcarbodiimide (DIPCDI)/hydroxybenzotriazole (HOBt)-mediated coupling which was used for the other residues. However, this could not completely suppress the formation of some dehydrated product (approximately 10%) which could be easily separated by column chromatography. After purification, **OPV-2** was obtained in 28% yield. The chemical structure of **OPV-1** was confirmed by ^{1}H and ^{13}C NMR spectroscopy and matrix-assisted laser desorption/ionization time-of-flight mass spectrometry (MALDI-TOF MS), while **OPV-2** was characterized by ^{1}H NMR spectroscopy and electrospray mass spectrometry (ESI MS).[29] It was not possible to measure a ^{13}C NMR spectrum of **OPV-2** due to its poor solubility.

The two different strategies that we have applied to synthesize the OPV−peptide conjugates have their own advantages. The solid-phase strategy enables us to use longer peptides as long as no strong acidic conditions are needed to deprotect the peptide and to get it from the resin. The solution-phase coupling gives apart from the soft reaction conditions a better yield (62%) compared to the solid-phase coupling reaction (28%).

Self-Assembly at the Liquid−Solid Interface. Scanning tunneling microscopy (STM) was used to study the 2D self-assembly of **OPV-1** and **OPV-2** at the liquid−solid interface in order to obtain direct visual evidence for the ability of the OPV−peptides to assemble into rows adopting a β-sheet conformation. STM is known to reveal the structure of physisorbed self-assembled molecular patterns with submolecular resolution and gives invaluable insight in the possible supramolecular interactions. Highly oriented pyrolytic graphite (HOPG) was used as solid support since it has proven to be an ideal substrate for the physisorption of (alkylated) organic molecules; it is conductive, atomically flat, chemically inert, and easy to work with.[31] First, 1-phenyloctane was used; however, in case

(5) (a) Klok, H.-A.; Lecommandoux, S. *Adv. Polym. Sci.* **2006**, *202*, 75. (b) Klok, H.-A. *J. Polym. Sci., Part A: Polym. Chem.* **2005**, *43*, 1. (c) Vandermeulen, G. W. M.; Klok, H.-A. *Macromol. Biosci.* **2004**, *4*, 383.

(6) For reviews on peptide based amphiphiles see: (a) Löwik, D. W. P. M.; van Hest, J. C. M. *Chem. Soc. Rev.* **2004**, *33*, 234. (b) Kokkoli, E.; Mardilovich, A.; Wedekind, A.; Rexeisen, L. E.; Garg, A.; Craig, J. A. *Soft Matter* **2006**, *2*, 1015.

(7) Pagel, K.; Vagt, T.; Koksch, B. *Org. Biomol. Chem.* **2005**, *3*, 3843.

(8) (a) Mart, R. J.; Osborne, R. D.; Stevens, M. M.; Ulijn, R. V. *Soft Matter* **2006**, *2*, 822. (b) Lim, Y.-b.; Lee, M. *J. Mater. Chem.* **2008**, *18*, 723. (c) Rajagopal, K.; Schneider, J. P. *Curr. Opin. Struct. Biol.* **2004**, *14*, 480. (d) Shimizu, T.; Masuda, M.; Minamikawa, H. *Chem. Rev.* **2005**, *105*, 1401. (e) van Hest, J. C. M. *J. Macromol. Sci., Polym. Rev.* **2007**, *47*, 63.

(9) Gazit, E. *Chem. Soc. Rev.* **2007**, *36*, 1263.

(10) (a) Hoeben, F. J. M.; Jonkheijm, P.; Meijer, E. W.; Schenning, A. P. H. J. *Chem. Rev.* **2005**, *105*, 1491. (b) Schenning, A. P. H. J.; Meijer, E. W. *Chem. Commun.* **2005**, 3245. (c) Watson, M. D.; Fechtenkötter, A.; Müllen, K. *Chem. Rev.* **2001**, *101*, 1267–1300. (d) Grimsdale, A. C.; Müllen, K. *Angew. Chem., Int. Ed.* **2005**, *44*, 5592–5629. (e) Wu, J.; Pisula, W.; Müllen, K. *Chem. Rev.* **2007**, *107*, 718–747. (f) Schenning, A. P. H. J. *Synth. Met.* **2004**, *147*, 43.

(11) (a) Jonkheijm, P.; van der Shoot, P.; Schenning, A. P. H. J.; Meijer, E. W. *Science* **2006**, *313*, 80. (b) Jonkheijm, P.; Hoeben, F. J. M.; Kleppinger, R.; van Herrikhuyzen, J.; Schenning, A. P. H. J.; Meijer, E. W. *J. Am. Chem. Soc.* **2003**, *125*, 15941.

(12) (a) Nilsson, K. P. R.; Rydberg, J.; Baltzer, L.; Inganäs, O. *Proc. Natl. Acad. Sci. U.S.A.* **2003**, *100*, 10170. (b) Nilsson, K. P. R.; Rydberg, J.; Baltzer, L.; Inganäs, O. *Proc. Natl. Acad. Sci. U.S.A.* **2004**, *1010*, 11197.

(13) Frauenrath, H.; Jahnke, E. *Chem. Eur. J.* **2008**, *14*, 2942.

(14) (a) Thoma, S. W.; Joly, G. D.; Swager, T. M. *Chem. Rev* **2007**, *107*, 1339. (b) Herland, A.; Inganäs, O. *Macromol. Rapid Commun.* **2007**, *28*, 1703.

(15) Hamley, I. W. *Angew. Chem., Int. Ed.* **2007**, *46*, 8128.

(16) (a) Kong, X.; Jenekhe, S. A. *Macromolecules* **2004**, *37*, 8180. (b) Rubatat, L.; Kong, X.; Jenekhe, S. A.; Ruokolainen, J.; Hojeij, M.; Mezzenga, R. *Macromolecules* **2008**, *41*, 1846.

(17) Klok, H.-A.; Rösler, A.; Götz, G.; Mena-Osteritz, E.; Bäuerle, P. *Org. Biomol. Chem.* **2004**, *2*, 3541.

(18) Harrington, D. A.; Behanna, H. A.; Tew, G. N.; Claussen, R. C.; Stupp, S. I. *Chem. Biol.* **2005**, *12*, 1085.

(19) Gong, J.-R.; Yan, H.-J.; Yuan, Q.-H.; Xu, L.-P.; Bo, Z.-S.; Wan, L.-J. *J. Am. Chem. Soc.* **2006**, *128*, 12384.

(20) For examples on peptide assemblies with a conjugated polydiacetylene backbone see: (a) Biesalski, M.; Tu, R.; Tirrell, M. V. *Langmuir* **2005**, *21*, 5663. (b) Biesalski, M. A.; Knaebel, A.; Tu, R.; Tirrell, M. V. *Biomaterials* **2006**, *27*, 1259. (c) Löwik, D. W. P. M.; Shklyarevskiy, I. O.; Ruizendaal, L.; Christianen, P. C. M.; Maan, J. C.; van Hest, J. C. M. *Adv. Mater.* **2007**, *19*, 1191. (d) Jahnke, E.; Lieberwirth, I.; Severin, N.; Rabe, J. P.; Frauenrath, H. *Angew. Chem., Int. Ed.* **2006**, *45*, 5383. (e) Hsu, L.; Cvetanovich, G. L.; Stupp, S. I. *J. Am. Chem. Soc.* **2008**, *130*, 3892.

(21) Bull, S. R.; Palmer, L. C.; Fry, N. J.; Greenfield, M. A.; Messmore, B. W.; Meade, T. J.; Stupp, S. I. *J. Am. Chem. Soc.* **2008**, *130*, 2742.

(22) (a) Wosnick, J. H.; Mello, C. M.; Swager, T. M. *J. Am. Chem. Soc.* **2005**, *127*, 3400. (b) Behanna, H. A.; Rajangam, K.; Stupp, S. I. *J. Am. Chem. Soc.* **2007**, *129*, 321. (c) Åslund, A.; Herland, A.; Hammerström, P.; Nilsson, K. P. R.; Jonsson, B.-H.; Inganäs, O.; Konradsson, P. *Bioconjugate Chem.* **2007**, *18*, 1860.

(23) For examples on dye−peptide conjugates see: (a) Gabriel, G. J.; Iverson, B. L. *J. Am. Chem. Soc.* **2002**, *122*, 15174. (b) Matsuzawa, Y.; Ueki, K.; Yoshida, M.; Tamaoki, N.; Nakamura, T.; Sakai, H.; Abe, M. *Adv. Funct. Mater.* **2007**, *17*, 1507. (c) Dunetz, J. R.; Sandstrom, C.; Young, E. R.; Baker, P.; van Name, S. A.; Cathopolous, T.; Fairman, R.; De Paula, J. C.; Kerfeldt, K. S. *Org. Lett.* **2005**, *7*, 2559. (d) Sibrian-Vazquez, M.; Jensen, T. J.; Fronczek, F. R.; Hammer, R. P.; Vicente, M. G. H. *Bioconjugate Chem.* **2005**, *16*, 852. (e) Arai, T.; Inudo, M.; Ishimatsu, T.; Akamatsu, C.; Tokusaki, Y.; Sasaki, T.; Nishino, N. *J. Org. Chem.* **2003**, *68*, 5540.

(24) (a) Jonkheijm, P.; Miura, A.; Zdanowska, M.; Hoeben, F. J. M.; De Feyter, S.; Schenning, A. P. H. J.; De Schryver, F. C.; Meijer, E. W. *Angew. Chem., Int. Ed.* **2004**, *43*, 74. (b) Gesquière, A.; Jonkheijm, P.; Schenning, A. P. H. J.; Mena-Osteritz, E.; Bäuerle, P.; De Feyter, S.; De Schryver, F. C.; Meijer, E. W. *J. Mater. Chem.* **2003**, *13*, 2164. (c) Gesquière, A.; Jonkheijm, P.; Hoeben, F. J. M.; Schenning, A. P. H. J.; De Feyter, S.; De Schryver, F. C.; Meijer, E. W. *Nano Lett.* **2004**, *4*, 1175.

(25) van Hest, J. C. M.; Tirrell, D. A. *Chem. Commun.* **2001**, 1897.

(26) Cerami, C.; Frevert, U.; Sinnis, P.; Takacs, B.; Clavijo, P.; Santos, M. J.; Nussenzweig, V. *Cell* **1992**, *70*, 1021.

(27) (a) Robinson, J. A. *Synlett* **1999**, *4*, 429. (b) Moreno, R.; Jiang, L.; Moehle, K.; Zurbriggen, R.; Glück, R.; Robinson, J. A.; Pluschke, G. *ChemBioChem* **2001**, *2*, 838. (c) Bisang, C.; Jiang, L.; Freund, E.; Emery, F.; Bach, C.; Matile, H.; Pluschke, G.; Robinson, J. A. *J. Am. Chem. Soc.* **1998**, *120*, 7439.

(28) (a) Löwik, D. W. P. M.; Linhardt, J. G.; Adams, P. J. H. M.; van Hest, J. C. M. *Org. Biomol. Chem.* **2003**, *1*, 1827. (b) Löwik, D. W. P. M.; Garcia-Hartjes, J.; Meijer, J. T.; van Hest, J. C. M. *Langmuir* **2005**, *21*, 524. (c) Löwik, D. W. P. M.; Shklyarevskiy, I. O.; Ruizendaal, L.; Christianen, P. C. M.; Maan, J. C.; van Hest, J. C. M. *Adv. Mater.* **2007**, *19*, 1191.

(29) See the Supporting Information.

(30) (a) Atherton, E.; Sheppard, R. C. *Solid Phase Peptide Synthesis*; IRL Press: Oxford, U.K., 1989. (b) Fields, G. B.; Noble, R. L. *Int. J. Pept. Protein Res.* **1990**, *35*, 161.

(31) (a) Rabe, J. P.; Buchholz, S. *Science* **1991**, *253*, 424. (b) Cyr, D. M.; Venkataraman, B.; Flynn, G. W. *Chem. Mater.* **1996**, *8*, 1600. (c) De Feyter, S.; De Schryver, F. C. *J. Phys. Chem. B* **2005**, *109*, 4290.

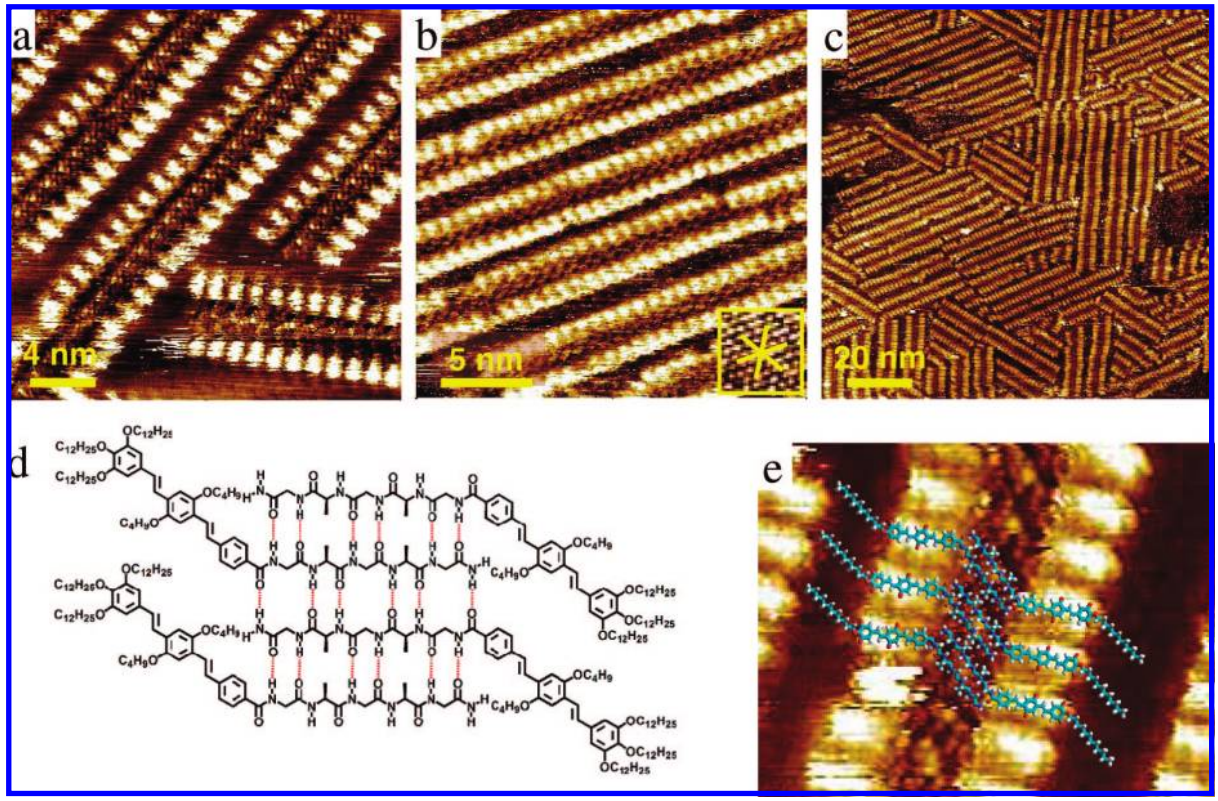

Figure 1. (a−c) STM images of **OPV-1** at the 1-octanoic acid−HOPG interface. $I_{set} = 0.028$ nA, $V_{set} = -0.860$ V. (b) Inset: underlying graphite and three main symmetry axes. (d) Molecular structure of an antiparallel β-sheet conformation of an **OPV-1** monolayer. (e) Zoom of image (a) with a superimposed molecular model.

of **OPV-2** no stable monolayers were observed probably due to its poor solubility in this solvent. **OPV-1** formed disordered monolayers, and in some cases, on top of these monolayers fibers were observed. Optical studies showed that **OPV-1** molecules are self-assembled in phenyloctane which was supported by atomic force microscopy (AFM) studies.[29] For getting ordered monolayers a solvent is preferred in which the molecules are molecularly dissolved. Hence, 1-octanoic acid was chosen as the solvent because it is capable of forming hydrogen bonds with our OPV−peptide conjugates thereby weakening the formation of aggregates in solution and facilitating the adsorption at the liquid−solid interface.[32] In case of **OPV-2** again no monolayer could be observed presumably because this molecule is aggregated in 1-octanoic acid (vide infra). STM images of **OPV-1** show the formation of bilayer-like supramolecular structures (Figure 1). These structures consist of **OPV-1** molecules that are stacked antiparallel next to each other. Each bilayer contains three rows in which the bright rods correspond to the OPV part (highest tunneling efficiency) of **OPV-1**, whereas the darker line in between is related to the peptide part.[33] The peptide backbone is probably fully extended on the graphite forming a β-strand of which successive strands are forming an antiparallel β-sheet held together by six hydrogen bonds (Figure 1d). This assumption is supported by infrared (IR) spectroscopy on a powder sample of **OPV-1** which shows that indeed such an organization is possible. The IR spectrum shows the amide I carbonyl stretching vibration at 1625 cm^{-1} with a shoulder at 1695 cm^{-1} and the amide II band at 1535 cm^{-1}, revealing a hydrogen-bonded antiparallel β-sheet secondary structure of the peptide segments.[5,29] The STM images show that the growth of the bilayers is one-dimensionally driven following the three main symmetry axes of graphite (Figure 1b), i.e., the equivalent $\langle 1\ -2\ 1\ 0 \rangle$ directions. Typically, the registry of the monolayer versus the graphite substrate is evaluated by recording an image of the graphite substrate (obtained at a smaller bias voltage) on the same location immediately after or before recording a monolayer image (see also the Supporting Information for a histogram reflecting the angle between the bilayer rows and a main symmetry axes of graphite).

The distance between neighboring rows (the dark troughs) varies from 1.6 to 2.8 nm. Here, the alkyl chains of the tridodecyloxybenzene end groups are located although they cannot be visualized by STM probably because they are too mobile. This variation in interbilayer distances can be understood in terms of differences in interactions between the alkyl chains, being fully, partially, or not interdigitated.[29] Note that it is not feasible for all alkyl chains to be adsorbed on the substrate in case they are interdigitated.

Analysis of the dimensions of the structures observed in the STM images shows that the model (Figure 1, parts d and e) fits very well with the results obtained. The width of a bilayer, omitting the alkyl tails, is 5.1 ± 0.1 nm, and the distance between different OPV units is 1.20 ± 0.05 nm, while the angle between the OPV and the peptide part is 157° ± 2°.

Self-Assembly in Solution. We have further studied the self-assembly of our OPV−peptide conjugates in solution by optical

(32) (a) Schurrmans, N.; Uji-i, H.; Mamdouh, W.; De Schryver, F. C.; Feringa, B. L.; van Esch, J.; De Feyter, S. *J. Am. Chem. Soc.* **2004**, *126*, 13884. (b) De Feyter, S.; Grim, K.; van Esch, J.; Kellogg, R. M.; Feringa, B. L.; De Schryver, F. C. *J. Phys. Chem. B* **1998**, *102*, 8981.
(33) Lazzaroni, R.; Calderone, A.; Brédas, J. L.; Rabe, J. P. *J. Chem. Phys.* **1997**, *107* (1), 99.

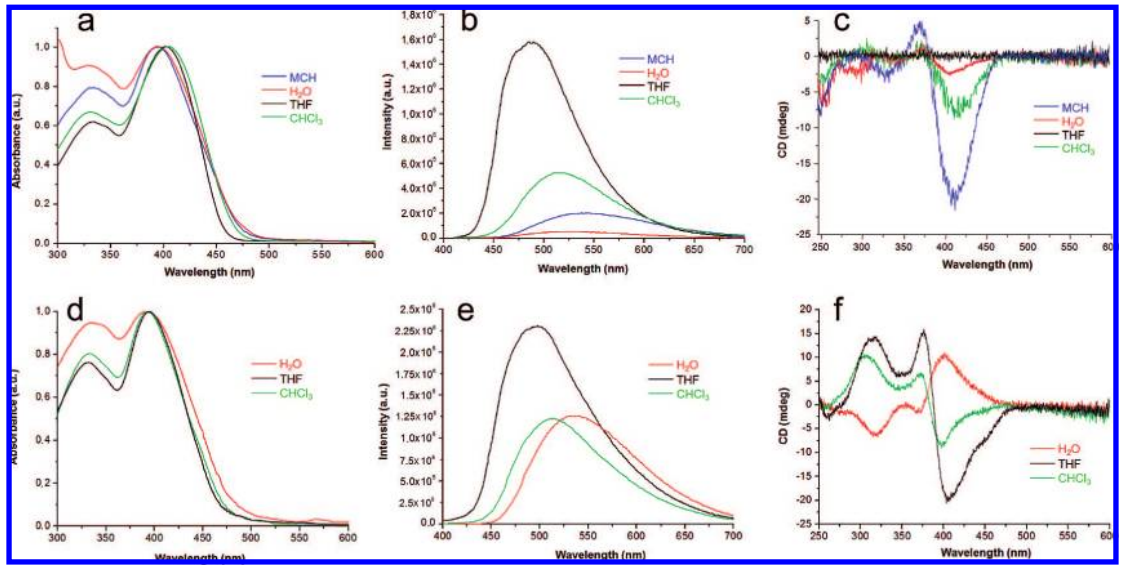

Figure 2. UV−vis (10^{-4} M, $T = 20$ °C), fluorescence ($\lambda_{exc} = 400$ nm, 10^{-5} M, $T = 20$ °C), and CD spectra (10^{-4} M, $T = 20$ °C) of **OPV-1** in THF, chloroform, MCH, and water (top panels) and UV−vis (10^{-4} M, $T = 20$ °C), fluorescence ($\lambda_{exc} = 400$ nm, 10^{-5} M, $T = 20$ °C), and CD spectra (10^{-4} M, $T = 20$ °C) of **OPV-2** in THF, chloroform, and water (bottom panels).

methods. Due to the amphiphilic nature of the compounds we have chosen solvents of different polarity, that is, methylcyclohexane (MCH), tetrahydrofuran (THF), chloroform, and water. In THF solution, **OPV-1** reveals very similar absorption ($\lambda_{max} = 400$ nm) and emission ($\lambda_{em,max} = 486$ nm) properties as those of the precursor **OPV−COOH** indicating that **OPV-1** is molecularly dissolved in THF (Figure 2). This suggests that in THF no hydrogen bonding takes place between the peptide segments. Similar optical characteristics have been reported for other molecular dissolved OPVs.[11] Aggregation is observed in chloroform ($CHCl_3$), MCH, and water with a red shift in the case of $CHCl_3$ ($\lambda_{max} = 405$ nm) and a blue shift in the cases of MCH ($\lambda_{max} = 390$ nm) and water ($\lambda_{max} = 389$ nm) (Figure 2a,d).[34] This behavior was confirmed by the fluorescence studies in the different solvents (Figure 2b,e). Indeed the fluorescence intensities obtained, using the same excitation wavelength ($\lambda_{exc} = 400$ nm) and the same optical density, were found to be much lower and red-shifted in $CHCl_3$ ($\lambda_{em,max} = 514$ nm), MCH ($\lambda_{em,max} = 542$ nm), and water ($\lambda_{em,max} = 531$ nm) than the one in THF ($\lambda_{em,max} = 486$ nm). Remarkably, **OPV-2** is already aggregated in THF indicated by the absorption maximum located at $\lambda_{max} = 394$ nm and the emission maximum at $\lambda_{em,max} = 500$ nm (Figure 2) and barely soluble in MCH. A blue shift in the absorption spectrum was observed in $CHCl_3$ ($\lambda_{max} = 392$ nm) and water ($\lambda_{max} = 392$ nm), whereas the fluorescence spectra exhibited weak emission intensities in $CHCl_3$ ($\lambda_{em,max} = 511$ nm) and water ($\lambda_{em,max} = 525$ nm) demonstrating aggregation in these solvents (Figure 2).

The conclusions drawn from the absorption/fluorescence studies on the aggregation behavior of **OPV-1** and **OPV-2** were strengthened by chiroptical spectroscopy studies (Figure 2c,f). Indeed, from the circular dichroism (CD) spectroscopy studies on **OPV-1** solutions CD effects could be observed in MCH and water with mainly negative Cotton effects indicating self-assembly of the OPV chromophores in contrast to the THF solution where **OPV-1** is molecularly dissolved (no CD signal) (Figure 2). A more careful characterization of the aggregation behavior of **OPV-1** by linear dichroism (LD) spectroscopy demonstrated that in $CHCl_3$ the CD signal is mainly a result of LD effects suggesting that large self-assembled objects are formed.[19,35] No LD was found in THF, MCH, or water revealing in this case helical self-assembly of the achiral OPV segments by the chiral peptide segments. In a similar manner, CD spectroscopy studies on solutions of **OPV-2** were in good agreement with the conclusion drawn from the absorption/fluorescence measurements. A bisignated Cotton effect is observed in THF with a negative sign at high wavelength and a zero crossing at $\lambda = 388$ nm that is close to the absorption maximum. A similar shape of the CD spectrum is measured in $CHCl_3$. Interestingly, a mirror image spectrum was observed in water suggesting that in this case the OPV chromophores are arranged in a right-handed helix. Unfortunately, due to the high absorption intensity in the UV region of the OPV chromophore, the conformation of the peptide could not be analyzed by CD (absorption below 240 nm).[36]

The spectroscopy studies show the large influence of the solvent on the optical properties of either **OPV-1** or **OPV-2**. Most likely the solvent polarity determines the self-assembly behavior of the OPV−peptide amphiphiles in a similar way as found for classical surfactant. Although we did not investigate the self-assembly in all solvents in detail (vide infra), most likely the hydrophilic peptide parts are located inside the aggregates in MCH, whereas they are positioned at the periphery in case of more polar solvents.[37] Our data show that the variation between molecular dissolution and aggregation in solution of OPV−peptide conjugates is a function of solvent chosen and

(34) de Cuendias, A.; Ibarboure, E.; Lecommandoux, S.; Cloutet, E.; Cramail, H. *J. Polym. Sci., Part A: Polym. Chem.* **2008**, *46*, 4602.

(35) Wolffs, M.; George, S. J.; Tomovic, Z.; Meskers, S. C. J.; Schenning, A. P. H. J.; Meijer, E. W. *Angew. Chem., Int. Ed.* **2007**, *46*, 8203.

(36) Kelly, S. M.; Jess, T. J.; Price, N. C. *Biochim. Biophys. Acta* **2005**, *1751*, 119.

(37) At the moment it is unclear what the main driving force is for aggregation. Beside the peptide and OPV part, it could well be that the trialkoxybenzene wedge also plays an important role; see, for example:(a) Balagurusamy, V. S. K.; Ungar, G.; Percec, V.; Johansson, G. *J. Am Chem. Soc,* **1997**, *119*, 1539. (b) Lecommandoux, S.; Klok, H.-A.; Sayar, M.; Stupp, S. I. *J. Polym. Sci., Part A: Polym. Chem.* **2003**, *41*, 3501.

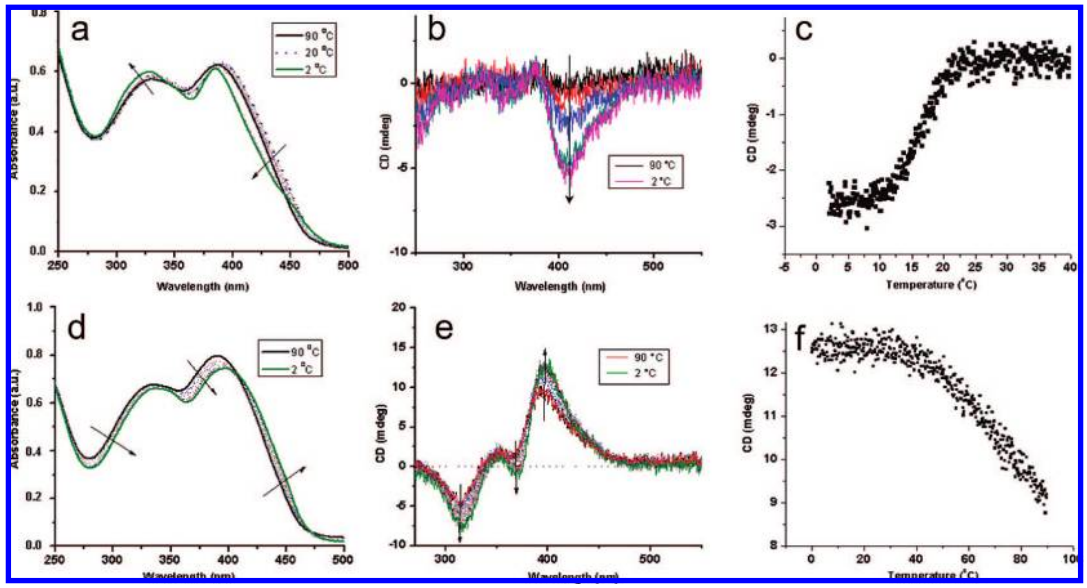

Figure 3. Temperature-dependent UV−vis and CD spectra of **OPV-1** (3.3×10^{-5} M, $T = 2-90$ °C) (top panels) and **OPV-2** (4×10^{-5} M, $T = 2-90$ °C) (bottom panels) in water. The arrows indicate changes upon cooling.

that optical properties of the assemblies can be manipulated by the polarity of the solvent.

We have investigated the self-assembly of **OPV-1** and **OPV-2** in aqueous solution in more detail. The self-assembly behavior was first studied as a function of the temperature by optical techniques (Figure 3). Upon cooling to room temperature, the UV−vis spectrum of **OPV-1** did not show significant changes, whereas a blue shift of the absorption maximum was observed upon further cooling. In the latter temperature regime also a CD effect appears (Figure 3). Fluorescence measurements showed nearly no increase in intensity, whereas a small change in the shape of the spectrum was observed at room temperature upon increasing the temperature.[29] This data suggests that a phase transition from chiral to achiral aggregates occurs at room temperature (vide infra). UV−vis absorption measurements on **OPV-2** showed a small red shift of the absorption maximum upon cooling, whereas the CD effect only slightly increased until 50 °C and remained constant below this temperature (Figure 3). Remarkably, also at 90 °C a CD effect was observed revealing that helical aggregates are still present at this temperature.

Our temperature-dependent optical data reveals that **OPV-1** behaves more as a classical amphiphile showing the typical sharp phase transition, whereas **OPV-2** shows a gradual transition in water.[38]

Light-scattering studies of **OPV-1** and **OPV-2** demonstrate in both cases the formation of cylindrical aggregates (Figure 4, parts A and B). In case of **OPV-1** the data could be fit assuming cylinders that are at least 1 μm long with an average diameter of 200 nm, whereas for **OPV-2** cylinders with an average length of 500 nm were obtained having a diameter of 150 nm. Temperature-dependent light-scattering measurements[29] did not reveal a change in shape and size of the assemblies indicating no breaking of the aggregates even at higher temperatures which confirms the results obtained by the temperature-dependent optical studies.

(38) Holmberg, K.; Jonsson, B.; Kronberg, B.; Lindman, B. *Surfactants and Polymers in Aqueous Solution*, 2nd ed.; John Wiley and Sons Ltd.: Chichester, England, 2003.

The supramolecular aggregates were further characterized by AFM microscopy after drop casting an aqueous solution on different type of substrates. In case of **OPV-1**, a network of bundled fibers of micrometer length and having a width up to 0.2 μm were observed on a mica surface (Figure 4C). The width and height of a single fiber in these bundles is approximately 10 nm.[29] On glass and HOPG substrates again a network of bundles fibers was observed showing that most probably these aggregates are also present in water.[29] In case of **OPV-2** a densely packed network of micrometer long bundles of fibers in which a single fiber has a width of 10 nm was observed (Figure 4D). Here again on different types of substrates similar feature were observed.[29] Cryogenic temperature transmission electron microscopy (cryo-TEM) studies confirm the presence of cylindrical aggregates. Fibers formed by **OPV-1** are bundled and form a densely packed network. The diameter of a single fiber is approximately 8 nm (Figure 4E). Also **OPV-2** forms nanofibers, in which an individual fiber has a diameter of 10 nm (Figure 4F). Interestingly, in some cases the contrast is higher at the walls of the fibers which most likely is caused by the π-conjugated OPV segments giving more scattering.[29] The cylindrical shape observed by AFM and cryo-TEM is in agreement with light-scattering measurements; however, there is a discrepancy between the dimensions obtained by the scattering and surface techniques which could be due to the clustering of the fibers. Furthermore for fitting the light-scattering data we have used a model assuming monodisperse assemblies.

On the basis of the data above we propose that both OPV peptide conjugates behave as peptide amphiphiles forming cylindrical micelles.[4,6] The diameter of these cylinders corresponds with 2 times the length of the OPV−peptide conjugates. Most likely, in these amphiphiles, the more hydrophilic peptide segments are facing toward the water, whereas the hydrophobic OPV parts are located inside the bilayer.[28] Although we were not able to determine the helical arrangement of the peptide

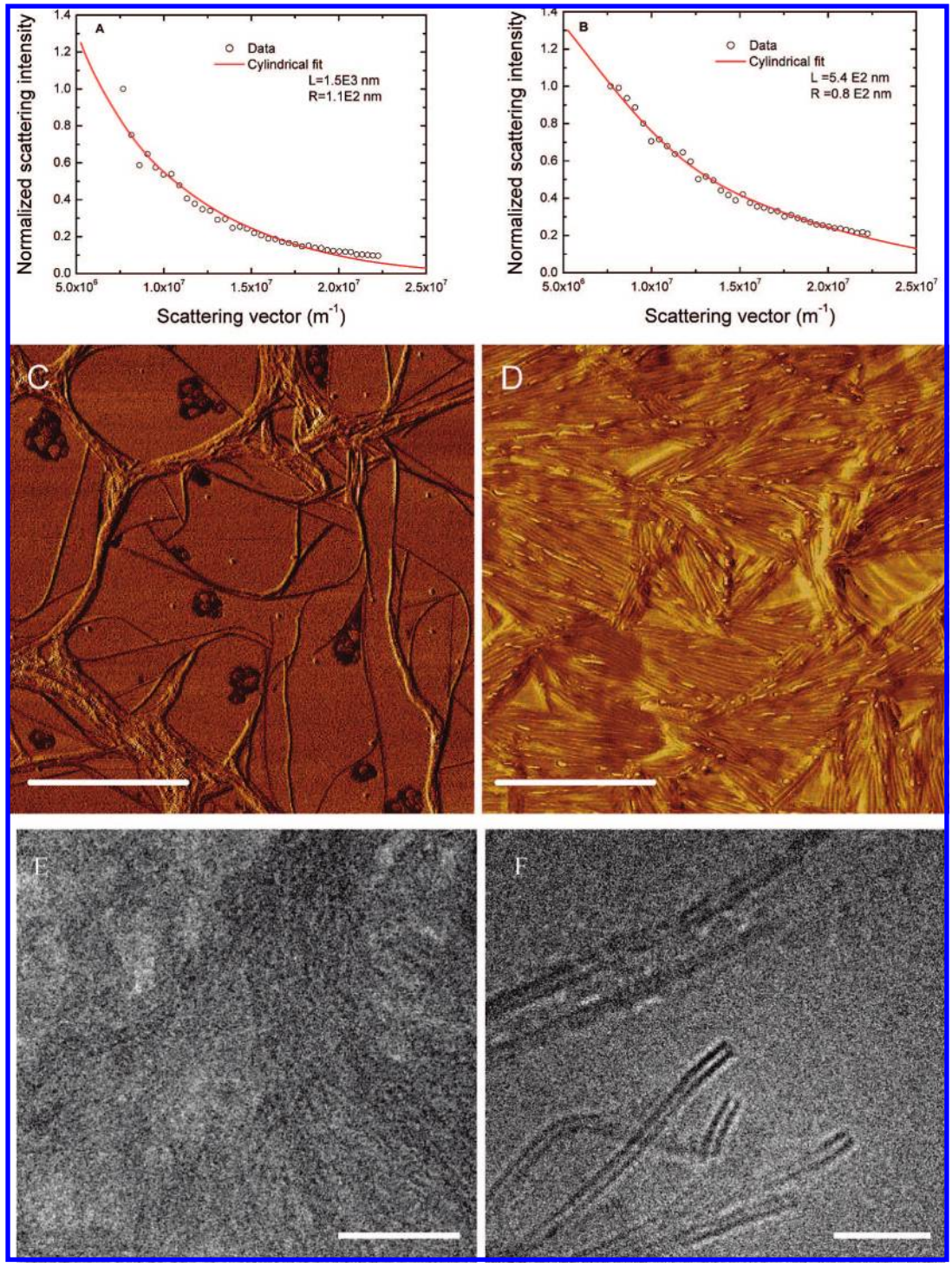

Figure 4. Light-scattering data of **OPV-1** (A) and **OPV-2** (B) in water ($C = 10^{-4}$ M), tapping mode AFM phase images of (C) **OPV-1** on freshly cleaved mica surface and (D) **OPV-2** on glass substrate (scale bar is 1.0 μm), and cryo-TEM images of **OPV-1** (E) and **OPV-2** (F) in water ($C = 10^{-5}$ M, scale bar is 50 nm).

segment we propose that both segments form β-sheets structures in which the peptide dictates the helical arrangement of the OPV segments.

Conclusion

We have developed synthetic routes to construct OPV-peptide conjugates based on a solid- and liquid-phase coupling reaction of a N-terminated amine and C-terminated amide GAGAG pentapeptide or a resin-bound GANPNAAG β-turn oligopeptide sequence with a carboxylic acid functionalized OPV derivative. These coupling strategies are efficient and versatile enough to be applied to any other peptide sequence possessing an amine function for the synthesis of a whole family of π-conjugated peptide conjugates. The characterization of the 2D self-assemblies of **OPV-1** by STM using graphite as a substrate demonstrated the formation of antiparallel β-sheet conformation and showed that the packing of π-conjugated segments is dictated by the peptide segment. The study of solution properties

of OPV−peptide hybrid materials by UV−vis and fluorescence spectroscopies showed strong aggregation of the OPV in a variety of solvents. The observations made from the absorption/fluorescence studies were confirmed by chiroptical spectroscopy. A more detailed analysis of the assemblies formed in water showed the formation of nanofibers in which the arrangement of the OPV segments is dictated by the peptide segment. Our results show that combining π-conjugated oligomers with peptides is an attractive approach to obtain an ordered 2D and 3D spatial organization of π-conjugated oligomers.

Acknowledgment. This work was supported by the EURYI scheme and the Council for Chemical Sciences of The Netherlands Organization for Scientific Research (CW-NWO). We thank Dr. Xianwen Lou for MALDI-TOF measurements. S.D.F. thanks the Fund for Scientific Research−Flanders and the Belgian Federal Science Policy Office via IAP-6/27. I.D.C. acknowledges financial support by IWT. P.L. is Chercheur Qualifié of the Fonds National de la Recherche Scientifique (FNRS−Belgium).

Supporting Information Available: Experimental details concerning the synthesis of **OPV−COOH**, **OPV-1**, and **OPV-2** and their characterization by ^{1}H and ^{13}C NMR, MALDI-TOF MS, ESI-MS, GPC, STM, AFM, DLS, and optical techniques. This material is available free of charge via the Internet at http://pubs.acs.org.

JA803026J